Jurnal Elektronika dan Telekomunikasi (JET), Vol. 25, No. 2, December 2025, pp. 119-125
Accredited by RISTEKDIKTI, Decree No: **158/E/KPT/2021**
doi: 10.55981/jet.798

Smartphone-Based Colorimetric Platform with RGB-CIELAB Multivariate Regression and 3D-Printed Illumination for Portable Colorimetric Detection

Robeth Viktoria Manurung[a*], Jonathan Edwards Telaumbanua[b], Richard Anthony Lim[b], Winda Astuti[b], Dedi[a], Agustina Sus Andreani[c]

[a]Research Center for Electronics
National Research and Innovation Agency, Republic of Indonesia
KST Samaun Samadikun, Jl. Cisitu No.21/154D
Bandung, Indonesia
[b]Automotive and Robotics Program, Computer Engineering Department,
BINUS ASO School of Engineering, Bina Nusantara University,
Jakarta, Indonesia 11480
[c]Research Center for Chemistry, National Research and Innovation Agency (BRIN),
PUSPIPTEK, Build. 452, Serpong, South Tangerang, 15314
Banten, Indonesia

Abstract

Smartphone-based colorimetry has become an effective alternative to bulky, costly spectrophotometers, especially for portable and field-based analysis. This study aims to develop Colorizer, a modular smartphone-based colorimetric platform designed to deliver accurate and affordable measurements for environmental, chemical, and biomedical uses. The system integrates a custom Android app with a 3D-printed sampling station that features controlled LED lighting, RGB-to-CIELAB conversion, calibration blanking, and multivariate regression modeling to ensure consistent results across devices. Illumination is controlled by an ESP32 microcontroller and activated via Bluetooth within a light-tight chamber to minimize ambient interference. Additional validation includes measuring multiple concentrations, benchmarking against standard spectrophotometers, and calibrating across different smartphones. Results indicate that Colorizer maintains high linearity across red, yellow, and blue dyes (R^2 up to 0.9952), shows improved stability with the sampling station, and aligns well with spectrophotometric calibration curves. These findings demonstrate that the platform offers reproducible, portable performance while functioning fully offline with local calibration storage. Colorizer provides a practical, low-cost alternative to benchtop spectrophotometers for routine colorimetric analysis. The platform presents a compact, scalable framework for portable analyte detection and sets the stage for future expansion into multi-indicator sensing applications.

Keywords: Controlled Illumination, Digital Image Colorimetry, Low-Cost Diagnostics, Multivariate Regression, Point-of-Care Testing, Portable Analytical Devices, Smartphone-based Colorimetry.

I. INTRODUCTION

Colorimetric assays are a fundamental technique in chemical analysis, biomedical testing, and environmental monitoring, relying on the measurement of color changes to quantify analyte concentrations with a rapid and cost-effective approach [1]–[6]. These assays operate by leveraging the interaction of analytes with specific reagents to produce detectable color shifts, which can be visually interpreted or measured to determine concentration levels, offering simplicity and minimal reagent requirements. Conventional spectrophotometers serve as the gold standard for such measurements, using precise optical systems to measure absorbance across a broad wavelength range with high reliability [3]–[5], [7]. However, these instruments are characterized by their bulky design, significant weight, and lack of portability, restricting their application to well-equipped laboratory settings and necessitating the use of alternatives for field-based applications [8]–[13].

Recent advances in smartphone imaging and processing capabilities have positioned mobile devices as viable tools for portable colorimetric analysis. High-resolution cameras, integrated sensors, and on-device computation allow smartphones to capture and process images for quantitative measurements in real time. Additionally, smartphones provide a widely accessible platform capable of supporting diverse analytical applications without specialized laboratory equipment. These advantages have motivated the development of a growing number of smartphone-based solutions for chemical and biomedical testing.

Despite this promise, smartphone-based colorimetric platforms still face persistent technical and practical challenges. Accuracy is frequently compromised by ambient light interference, device-to-device camera variation, and inconsistent image-processing pipelines [9]–[11]. Strategies such as flash/no-flash subtraction [9], ring-light modules [11], and background correction algorithms [14] have been introduced to mitigate these

* Corresponding Author.
Email: robeth.viktoria.manurung@brin.go.id
Received: September 8, 2025 ; Revised: October 23, 2025
Accepted: November 27, 2025 ; Published: December 31, 2025

factors. Other works have emphasized the importance of device-independent calibration and robust color-space transformations, such as HSV and CIELAB, to improve reproducibility across platforms [15]-[17].

Researchers have also investigated hardware-based methods, including 3D-printed holders, enclosed chambers, and optical diffusers, to stabilize imaging conditions [19], [20]. Meanwhile, cloud-based pipelines and AI-driven algorithms have been suggested to improve sensitivity and specificity, though these raise concerns about connectivity, privacy, and computational requirements [12], [21]. Overall, these advancements demonstrate a widespread and ongoing effort to develop portable, reliable, and affordable colorimetric systems using consumer devices.

In this work, we present Colorizer, a smartphone-based platform for fully offline colorimetric analysis. The system integrates RGB-to-CIELAB conversion, calibration blanking, and multivariate regression to reduce device variability. Validation experiments using synthetic dye assays evaluated accuracy, reproducibility, and cross-device performance. By combining controlled illumination in a 3D-printed chamber with modular software and hardware integration, the platform provides a compact and scalable solution suitable for environmental monitoring, education, routine assays, and potential point-of-care applications.

II. Experimental Method

A. System Design

The Colorizer platform is built on the principle of modularity, where software, hardware, and illumination are regarded as separate yet closely integrated subsystems. This design allows each module to be developed, optimized, and upgraded independently, without requiring a complete redesign. The platform comprises three main parts: (i) a smartphone app for capturing and processing images, (ii) a 3D-printed sampling station that guarantees consistent positioning and light isolation, and (iii) an ESP32-based microcontroller that manages a high-power LED for steady illumination. By integrating these modules, the platform offers portability, reproducibility, and independence from offline connectivity, overcoming key limitations of traditional spectrophotometers and earlier smartphone-based systems.

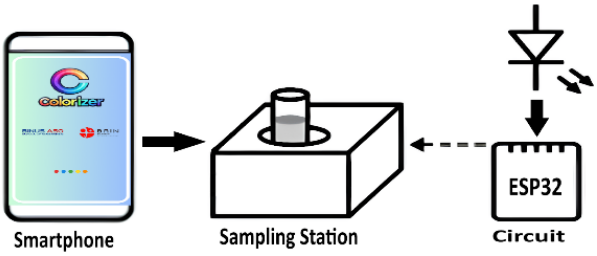

Figure 1. System architecture of colorizer.

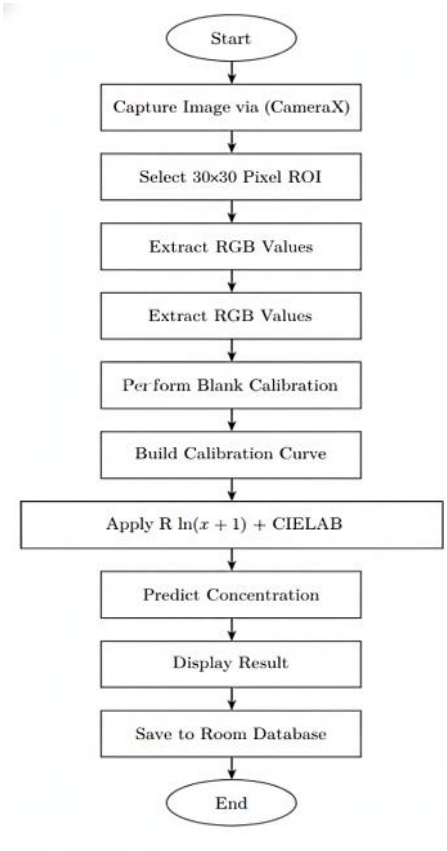

Figure 2. Operational workflow.

The overall system architecture is illustrated in Figure 1, showing the integration of smartphone software, the 3D-printed sampling station, and ESP32-controlled illumination.

A high-level operational workflow is presented in Figure 2, where samples are introduced into the cuvette holder, the smartphone captures images under controlled illumination, RGB values are transformed into CIELAB coordinates, calibration is applied, and multivariate regression generates analyte concentration predictions. This modular workflow demonstrates how the platform achieves a balance of low-cost design, reproducibility, and offline capability, distinguishing it from both traditional laboratory instrumentation and previous smartphone-based solutions.

B. Software Pipeline

The Colorizer smartphone app serves as the core of the platform, managing image capture, pre-processing, color adjustments, calibration blanking, and concentration prediction. It was built in Kotlin using Android Studio with the CameraX API, which offers precise control over settings such as ISO, exposure, and focus. Images were standardized to 480 × 640 pixels to optimize processing speed and image quality. This ensures compatibility with low- to mid-range smartphones often used in resource-limited settings.

For each captured image, a 30 × 30 pixel region of interest (ROI) was extracted from the center of the cuvette's optical path. Larger ROIs were avoided because they caused edge reflections, while smaller ROIs were more susceptible to random sensor noise. Averaging across 900 pixels reduced variability while maintaining

sensitivity to concentration changes, thereby improving overall measurement stability. ROI-based averaging has also been shown in previous smartphone colorimetric systems to enhance robustness against pixel noise [22]-[24].

The mean RGB values were then transformed into the CIELAB color space, which provides perceptual uniformity and reduces dependence on device-specific color profiles [25]. The conversion was performed using the standard RGB→XYZ→CIELAB transformation under a D65 illuminant, yielding L^*, a^*, and b^* values. These values, combined with the original RGB channels, formed a six-dimensional feature vector [R, G, B, L^*, a^*, b^*]. The process is illustrated in Figure 3, where blank calibration offsets are also applied.

$$y = \beta_0 + \sum_{i=1}^{n} \beta_i ln(x_i + 1) + \epsilon \quad (1)$$

Concentration prediction was carried out using multivariate linear regression (MLR) with log-transformed input features as described in (1). In (1), y represents the predicted concentration, β_0 is the intercept term, β_i denotes the regression coefficient for the *i-th* color feature, n represents the total number of color features ($n = 6$, corresponding to RGB and CIELAB color parameters), x_i refers to the *i-th* independent variable (raw color values: r, g, b, L, a, b), and ε is the error term accounting for residual variation not captured by the model. The log transform, $ln(x+1)$, was chosen to linearize the relationship between absorbance intensity and concentration, especially at higher levels. Ridge regularization with a penalty factor $\lambda = 0.01$ was used to reduce multicollinearity among color channels, stabilize coefficient estimates, and enhance reproducibility.

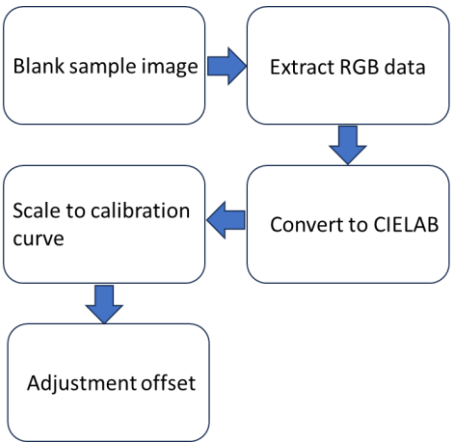

Figure 3. Offset adjustment.

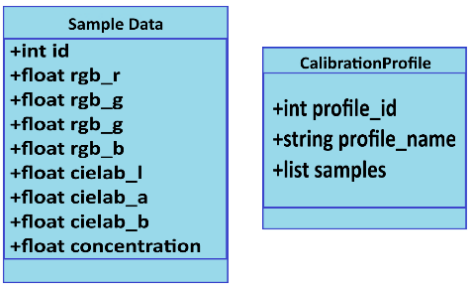

Figure 4. Room database.

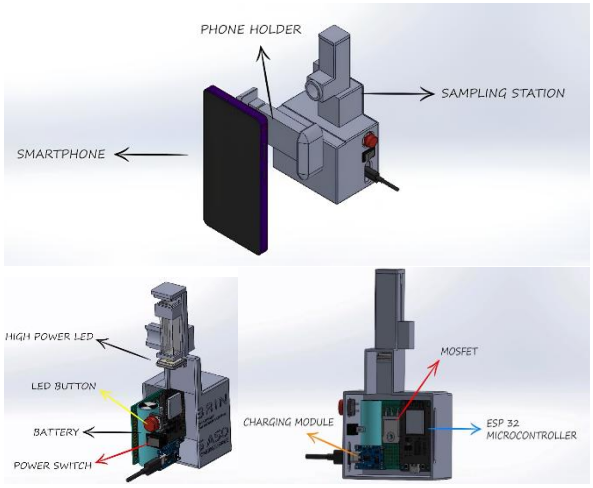

Figure 5. 3D-schematic ilustration of the Sampling Station .

All calibration data, regression coefficients, and measurement records were stored in an offline Room database (Figure 4). The schema includes tables for calibration entries, measurement history, and regression parameters, enabling persistent storage of calibration curves across sessions. This design ensures full operability in field conditions without internet access, supporting long-term monitoring where data continuity is essential. By decentralizing storage, the system guarantees transparency, reproducibility, and independence in resource-limited environments.

C. Hardware Configuration

The 3D-printed sampling station, made from PLA filament, was designed to securely hold standard cuvettes and dual smartphones for stable image capture. Its modular design includes a cuvette holder, a light-tight enclosure, and a rear cover to protect internal electronics while allowing easy maintenance (Figure 5). The station ensures precise positioning of both samples and cameras, maintaining consistent alignment during imaging. This design improves reproducibility and reduces external light interference, both of which are essential for accurate colorimetric measurements [19], [20].

A high-power LED provides illumination, carefully positioned to ensure even lighting across the cuvette. The LED is controlled by an ESP32 microcontroller, which manages timing and brightness, while power is supplied by a compact Li-ion battery for portability. The station includes basic circuit-stabilization components to prevent fluctuations during measurements, ensuring consistent data. Overall, this hardware setup creates a controlled, repeatable imaging environment, providing a solid foundation for accurate analysis.

D. Experimental Setup

Experiments were conducted using synthetic dye solutions (red, yellow, and blue) prepared at concentrations ranging from 0–100% in 10% increments, following Lambert-Beer law principles for absorbance-based quantification [3]–[5]. Each sample was placed in a 4 mL cuvette within the 3D-printed sampling station, with smartphones aligned via integrated holders to ensure consistent ROI capture. To evaluate the effect of ambient light, a subset of cuvettes was measured outside the

station; results demonstrated that the station substantially improved measurement reproducibility without requiring specialized laboratory conditions for calibration, a bundle of known samples (one from each dye) was measured first, followed by three replicates ($n=3$) per concentration under controlled ambient light (<50 lux) and temperature (25±2°C).

The setup, depicted in Figure 6, integrates the smartphone and the sampling station to maintain consistent and reproducible measurement conditions.

Illumination was controlled either via Bluetooth through the ESP32 microcontroller or manually with a momentary push button, ensuring consistent lighting and fixed geometry across all trials. Images were captured at 480×640 resolution using the CameraX library. A 30×30 pixel ROI was extracted, averaged, and converted from RGB to CIELAB. The calibration and prediction pipeline uses this conversion to minimize device-specific variation. Regression models were trained separately for each dye using three-channel CIELAB inputs with an $ln(x+1)$ transformation to address non-linearities. Bluetooth communication, shown in Figure 7, enabled smooth interaction between the mobile application and microcontroller, supporting both system calibration and testing. This integrated setup enabled reliable, repeatable data collection under field-like conditions, reducing dependence on traditional laboratory infrastructure while maintaining measurement accuracy.

Figure 6. Experimental setup.

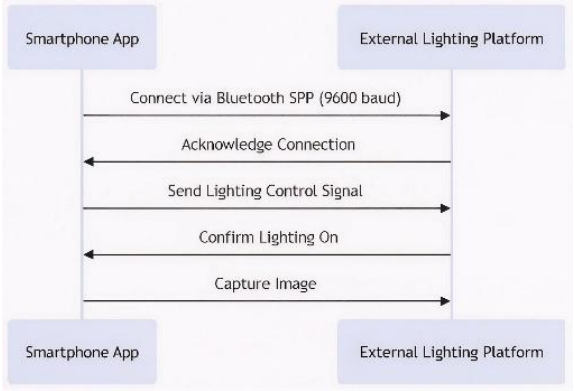

Figure 7. Bluetooth communication.

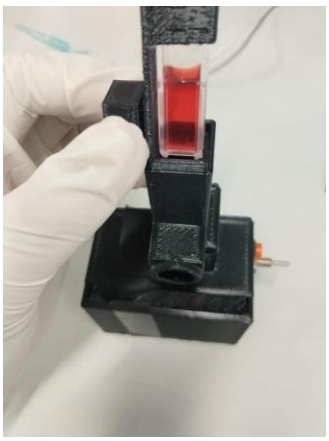

Figure 8. 3D-printed sampling station with cuvette.

III. Results

A. System Demonstration

The 3D-printed sampling station, made from PLA filament, effectively blocked ambient light from reaching the cuvette, preventing any interference during image capture. Comparative measurements with and without the station (Table I) showed a slight improvement in predictive accuracy when using the light-tight chamber. The chamber reliably held standard 4 mL cuvettes, keeping the samples stable across replicates, while built-in smartphone holders ensured accurate camera positioning. Its compact design and compatibility with standard cuvettes make it suitable for portable, field-based use (Figure 8).

The Android app captured images at 480×640 pixels using the CameraX library, targeting a 30×30-pixel ROI. Mean RGB values were extracted and converted to CIELAB coordinates in real time, with an average processing time of 500 ms per sample. Calibration blanking, normalized measurements, and MLR with $ln(x+1)$ transformation accurately predicted analyte concentrations. The bilingual interface (Indonesian-English) offered intuitive navigation and real-time readouts on the detection screen (Figure 9).

TABLE I
EFFECT OF SAMPLING STATION ON MEASURED CONCENTRATION

Dye Color	Concentration (%)		
	Actual	With Station (Avg $n=3$)	Without Station (Avg $n=3$)
Red	30	31.08	32.71
	70	70.15	71.26
	80	80.04	82.27
	90	90.30	92.67
Yellow	30	31.23	32.51
	70	72.04	73.35
	80	80.89	82.91
	90	91.72	93.07
Blue	30	32.42	34.61
	70	71.83	75.36
	80	83.01	85.94
	90	92.86	97.45

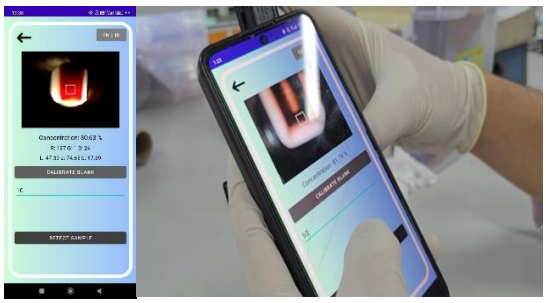

Figure 9. Colorizer app detection screen.

Illumination control, managed via an ESP32 microcontroller and a 1 W high-power LED, achieved less than 1% variance across replicates using Bluetooth Low Energy (BLE). Manual operation with a momentary push button was also supported for field flexibility. The 3.7 V Li-ion battery (≥1000 mAh) provided 15–20 minutes of continuous use. Hardware and software integration enabled seamless offline data collection, storage in a Room database, and immediate concentration predictions, confirming dependable performance under controlled conditions. With these operational conditions verified, the system's quantitative performance was assessed using synthetic-dye assays to evaluate predictive accuracy and reproducibility. The following section summarizes these results, emphasizing model performance with red, yellow, and blue dyes under the established measurement setup.

B. Performance Metrics

Validation experiments (Table II) using synthetic-dye assays demonstrated strong agreement between predicted and actual concentrations. The final regression models achieved R^2 values of 0.9952 for red, 0.9816 for yellow, and 0.9321 for blue, with corresponding Root Mean Square Error (RMSE) values of 1.901, 3.846, and 7.168. These metrics indicate high predictive accuracy for red and yellow dyes and slightly lower performance for blue due to reduced signal-to-noise ratios at higher absorbance levels. All measurements were performed in triplicate to ensure reproducibility.

TABLE II
PERFORMANCE METRICS FOR DYE ASSAYS

Dye Color	R^2	RMSE
Red	0.9952	1.901
Yellow	0.9816	3.846
Blue	0.9321	7.168

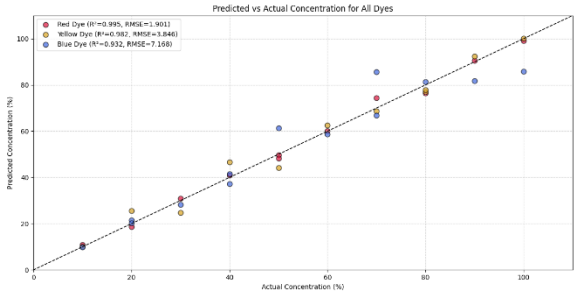

Figure 10. The calibration's curve of Predicted vs Actual Concentration of Dyes

System prediction modelling (Figure 10) provides a visual summary of the system's overall predictive performance by plotting predicted versus actual concentrations for all dyes. The regression curves closely follow the ideal 1:1 line, reflecting the strong linearity already indicated in Table II. Red and yellow dyes show tight clustering around the regression line, demonstrating high agreement across the whole concentration range. Blue dye data exhibit slightly wider dispersion, consistent with its lower R^2 and higher RMSE, but still maintain a clear linear trend.

The combined plots illustrate how the multivariate regression model generalizes across different colorimetric responses, confirming that the RGB-to-CIELAB transformation and illumination-controlled setup produce stable predictions suitable for portable analysis.

C. Comparative Reference Validation

Table III compares Colorizer's performance with the linear calibration fits from the reference spectrophotometer. This comparison determines whether the smartphone-based system exhibits the same concentration–absorbance performance as a laboratory-grade instrument.

Figure 11 visually reinforces these trends by showing the regression lines for both devices across the red, yellow, and blue assays. Red and yellow dyes displayed near-identical linearity between Colorizer and the spectrophotometer, with only minor deviations at higher concentrations. Blue dye measurements showed slightly larger dispersion yet maintained a consistent slope aligned with the reference curve. Together, Table III and Figure 11 confirm that Colorizer produces concentration predictions that are not only internally accurate but externally consistent with established spectrophotometric behavior.

These findings show that the controlled illumination chamber and CIELAB-based regression framework effectively minimize typical smartphone-related variability. The agreement with standard spectrophotometer curves enhances Colorizer's credibility as a portable analytical tool capable of approximating lab-grade measurements.

TABLE III
PERFORMANCE METRICS COMPARISON

Device	Metric	Red	Yellow	Blue
Spectrophotometer	R^2	1.00	0.984	0.987
Colorizer App	R^2	0.995	0.982	0.932

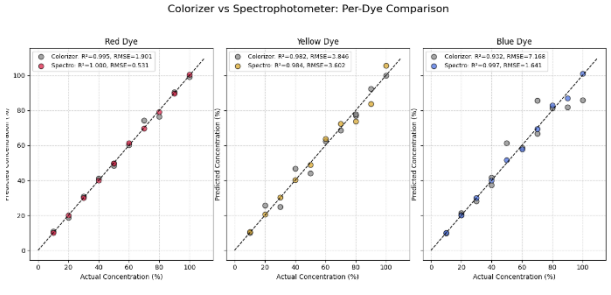

Figure 11. Colorizer vs spectrophotometer results comparison for each dye.

TABEL 1V
CROSS-DEVICE CALIBRATION TESTING

Dye Color	Concentration (%)				
	Actual	Poco F4 GT		Poco X5 5G	
		With Station	Without Station	With Station	Without Staton
Red	30	31.08	31.62	32.71	27.27
	70	70.15	71.26	71.26	73.97
	80	80.04	91.73	82.27	82.75
	90	90.30	91.24	92.13	92.67

D. Cross-Device Validation

Table IV presents cross-device testing between the Poco F4 and Poco X5 under both station and no-station conditions. Cross-device evaluation showed that measurements taken inside the illumination chamber exhibited minimal variation between smartphones. This confirms that the platform's fixed geometry, stable LED illumination, and RGB-to-CIELAB normalization successfully compensate for differences in sensor characteristics, white balance behavior, and image processing pipelines across devices. In contrast, no-station measurements showed larger deviations, reflecting the impact of uncontrolled ambient lighting and inconsistent positioning.

IV. DISCUSSION

The Colorizer platform showed strong reproducibility, portability, and analytical reliability across all tested dye assays. The controlled illumination chamber was key to this performance, maintaining stable optical conditions and reducing the impact of ambient light. Along with fixed smartphone positioning, this ensured consistent image capture across replicates and devices. These conditions directly contributed to the high R^2 values seen for red and yellow dyes in Table II and Figure 10, confirming that the measurement process remained linear across the tested concentration ranges.

The RGB-to-CIELAB transformation and $ln(x+1)$ feature adjustment further improved predictive accuracy by reducing device-specific variation and linearizing the color–concentration response. These lightweight processing steps were sufficient to achieve near-spectrophotometric agreement for red and yellow dyes, as shown in Table III and Figure 11. Blue dyes showed greater variance and higher RMSE, consistent with the inherent difficulty of quantifying darker samples using smartphone cameras. Despite this, the platform maintained an overall linear trend aligned with the reference instrument, indicating that the core modeling pipeline remains effective even under challenging optical conditions.

Cross-device comparisons in Table IV revealed that measurements taken inside the illumination chamber were consistent across smartphones. This shows that controlled lighting geometry helps reduce differences caused by sensor traits, automatic white balance, and internal image-processing pipelines. No-station testing exhibited noticeably larger deviations, highlighting the need for hardware stabilization to ensure accurate smartphone-based colorimetry. Overall, these results confirm that combining fixed geometry, stable illumination, and CIELAB normalization allows for consistent performance across various devices.

The offline architecture further improves the platform's field usability. Local calibration storage, on-device regression, and real-time processing enable operation without network connectivity, which is vital for remote or resource-limited settings. The small sampling station, Bluetooth-controlled illumination, and instant readout interface make the system ideal for environmental monitoring, educational labs, and emerging point-of-care workflows. The low hardware cost enhances accessibility in situations where benchtop spectrophotometers are impractical.

However, several limitations remain. Blue dye measurements showed reduced accuracy due to lower signal-to-noise ratios and partial sensor saturation at high absorbance levels. The experiments used synthetic dyes, which do not capture the complexity of real-world targets like environmental contaminants, biochemical markers, or food-quality indicators. The single-cuvette setup also limits throughput, making the system more suitable for low-volume testing. These limitations highlight opportunities for improved optical design, expanded calibration sets, and multi-sample or automated measurement formats.

Future development should concentrate on validation with actual analytes to evaluate performance in more complex matrices. Additional modeling techniques, such as partial least squares or lightweight neural networks optimized for mobile hardware, could improve prediction accuracy while maintaining real-time functionality. Broader benchmarking against established spectrophotometers and current smartphone colorimetry platforms will also be essential to understand Colorizer's accuracy, limitations, and practical benefits. Testing system robustness under varying lighting conditions, temperature changes, and sample turbidity will offer a more comprehensive view of operational limits. These efforts will drive iterative improvements to both hardware and software, leading to better optical stability, more flexible calibration processes, and potentially multi-analyte workflows. Overall, this will help evolve Colorizer into a dependable, field-ready tool for portable colorimetric measurement.

V. CONCLUSION

This study introduced Colorizer, a modular smartphone-based colorimetric platform that combines controlled LED lighting, RGB-to-CIELAB conversion, and lightweight multivariate regression for portable analyte measurement. The system demonstrated high reproducibility and closely matched the trends of the reference spectrophotometer for red and yellow dyes, thanks to stable illumination, a fixed imaging geometry, and device-independent color normalization. Although results for blue dye showed more variability due to sensor saturation and lower signal-to-noise ratios, the overall linear response across all dyes indicates that the measurement process is reliable under practical conditions. Cross-device testing revealed that the controlled illumination chamber significantly reduces variability among smartphones, highlighting the importance of optical stabilization in mobile colorimetry. Offline operation, local calibration storage, and real-time processing further enhance field usability, making the

platform suitable for environmental testing, educational purposes, and early-stage point-of-care workflows where traditional spectrophotometers are not available. Future work will extend validation to real analytes, including environmental contaminants, biochemical markers, and food-quality indicators, to evaluate performance in complex matrices. Additional improvements will investigate enhanced optical design, expanded calibration sets, and potential multi-sample formats to boost throughput. Further assessment of alternative modeling strategies, such as partial least squares regression or lightweight neural networks optimized for mobile devices, may enhance prediction accuracy while maintaining real-time operation. These developments will support the ongoing refinement of Colorizer as a reliable, scalable, and field-deployable platform for portable colorimetric analysis.

DECLARATIONS

Conflict of Interest

The authors declare no conflicts of interest that could potentially influence the research, data analysis, and interpretation.

CRediT Authorship Contribution

Robeth Viktoria Manurung: Writing – Review, Editing, Conceptualization, Methodology, Investigation, and Supervision; Jonathan Edwards Telaumbanua: Investigation, Data Curation, Writing - Original Draft, Visualization; Richard Anthony Lim: Design, Visualization, and Data Curation; Winda Astuti: Supervision. Methodology and Data Validation; Dedi: Investigation, Supervision Agustina Sus Andreani: Methodology and Reviewing.

Funding

This work was supported by the Riset dan Inovasi Untuk Indonesia Maju (RIIM) Fund Batch 3 project (SK DFRI-BRIN No.12/II.7/HK/2023). The authors also thank the Indonesia Endowment Fund for Education (Lembaga Pengelolaan Dana Pendidikan, or LPDP) for the research funding under RVM.

Acknowledgment

The authors thank the BASICS Advances Laboratories, Research, and Innovation Agency, Republic of Indonesia (BRIN) at KST Samaun Samadikun for supporting the research analysis.

REFERENCES

[1] Z. Jin et al., "Colorimetric sensing for translational applications: From colorants to mechanisms," *Chem. Soc. Rev.*, vol. 53, no. 15, pp. 7681–7741, 2024, doi: 10.1039/d4cs00328d.

[2] S. Krishnan and Z. ul Syed, "Colorimetric visual sensors for point-of-needs testing," *Sensors Actuators Rep.*, vol. 4, Nov. 2022, Art. no. 100078, doi: 10.1016/j.snr.2022.100078.

[3] A. K. Samanta, "Advanced methods and tools for color measuring and matching: for quality check of colored products of textiles and apparel industry," in *Advances in Colorimetry*, A. K. Samanta, Ed., IntechOpen, 2024, doi: 10.5772/intechopen.108083.

[4] Y. K. Shrestha and S. K. Shrestha, "Fundamentals of colorimetry," in *Advances in Colorimetry*, A. K. Samanta, Ed., IntechOpen, 2024, doi: 10.5772/intechopen.108083.

[5] S. Karuppaiah, N. Sermugapandian, S. Mohan, and M. Krishna, "Application of UV-visible spectrophotometric colour analysis in different natural product identification," in *Advances in Colorimetry*, A. K. Samanta, Ed., IntechOpen, 2024, doi: 10.5772/intechopen.108083.

[6] Y. Wu, J. Feng, G. Hu, E. Zhang, and H.-H. Yu, "Colorimetric sensors for chemical and biological sensing applications," *Sensors*, vol. 23, no. 5, Mar. 2023, doi: 10.3390/s23052749.

[7] Y. Xing et al., "A cellphone-based colorimetric multi-channel sensor for water environmental monitoring," *Front. Environ. Sci. Eng.*, vol. 16, no. 12, Jun. 2022, doi:10.1007/s11783-022-1590-z

[8] T. Kant et al., "Progress in the design of portable colorimetric chemical sensing devices," *Nanoscale*, vol. 15, no. 47, pp. 19016–19038, 2023. doi:10.1039/d3nr03803c

[9] M. Nixon, F. Outlaw, and T. S. Leung, "Accurate device-independent colorimetric measurements using smartphones," *PLoS One*, vol. 15, no. 3, Mar. 2020, doi: 10.1371/journal.pone.0230561.

[10] S. Balbach et al., "Smartphone-based colorimetric detection system for portable health tracking," *Anal. Methods*, vol. 13, no. 38, pp. 4361–4369, 2021, doi:10.1039/d1ay01209f.

[11] T. Sahare, B. N. Sahoo, S. Rana, and A. Joshi, "Smartphone-based colorimetric protein sensor platform utilizing an ambient ring light setup for urinary protein detection," *Microchem. J*, vol. 208, Jan. 2025, Art. no. 112527, doi:10.1016/j.microc.2024.112527.

[12] R. Mansour, C. Serafinelli, R. Jesus, and A. Fantoni, "Mobile platform for continuous screening of clear water quality using colorimetric plasmonic sensing," *Information*, vol. 16, no. 8, Aug. 2025, doi:10.3390/info16080683.

[13] H. Guan, S. Du, B. Han, Q. Zhang, and D. Wang, "A rapid and sensitive smartphone colorimetric sensor for detection of ascorbic acid in food using the nanozyme paper-based microfluidic chip," *LWT*, vol. 184, Jul. 2023, doi: 10.1016/j.lwt.2023.115043.

[14] G. M. S. Ross et al., "Best practices and current implementation of emerging smartphone-based (bio)sensors – part 1: Data handling and ethics," *TrAC Trends Anal. Chem.*, vol. 158, Jan. 2023, doi: 10.1016/j.trac.2022.116863.

[15] S. H. Elagamy, L. Adly, and M. A. A. Hamid, "Smartphone based colorimetric approach for quantitative determination of uric acid using image J," *Sci. Rep.*, vol. 13, no. 1, Dec. 2023, doi: 10.1038/s41598-023-48962-0.

[16] A. A. Ramírez-Coronel et al., "Smartphone-facilitated mobile colorimetric probes for rapid monitoring of chemical contaminations in food: Advances and outlook," *Crit. Rev. Anal. Chem.*, vol. 54, no. 7, pp. 2290–2308, 2024, doi:10.1080/10408347.2022.2164173.

[17] T. Gölcez, V. Kiliç, and M. Şen, "A portable smartphone-based platform with an offline image-processing tool for the rapid paper-based colorimetric detection of glucose in artificial saliva," *Anal. Sci.*, vol. 37, no. 4, pp. 561–567, Oct. 2020. doi:10.2116/analsci.20p262.

[18] T. Alawsi, G. P. Mattia, Z. Al-Bawi, and R. Beraldi, "Smartphone-based colorimetric sensor application for measuring biochemical material concentration," *Sens. Bio-Sens. Res.*, vol. 32, Jun. 2021, doi: 10.1016/j.sbsr.2021.100404.

[19] B. J. Winters et al., "3D-printable and open-source modular smartphone visible spectrophotometer," *HardwareX*, vol. 10, Oct. 2021, doi:10.1016/j.ohx.2021.e00232.

[20] T. Alawsi, Z. Albawi, R. Beraldi, G. P. Mattia, and R. Faris, "A custom 3D printed design of smartphone-based adapter for colorimetric biomarker concentration measurements," Jul. 2023, *OpticaOpen:107479*, doi:10.1364/opticaopen.23636244.v1.

[21] J. Chen et al., "Inclusive and accurate clinical diagnostics using intelligent computation and smartphone imaging," *ACS Sensors*, vol. 9, no. 10, pp. 5342–5353, Oct. 2024. doi:10.1021/acssensors.4c01588.

[22] A. Horta-Velázquez, G. Ramos-Ortiz, and E. Morales-Narváez, "The optimal color space enables advantageous smartphone-based colorimetric sensing," *Biosens. Bioelectron.*, vol. 273, Apr. 2025, Art. no. 117089, doi: 10.1016/j.bios.2024.117089.

[23] B. Coleman, C. Coarsey, M. A. Kabir, and W. Asghar, "Point-of-care colorimetric analysis through smartphone video," *Sens. Actuators B: Chem.*, vol. 282, pp. 225–231, Mar. 2019. doi: 10.1016/j.snb.2018.11.036.

[24] D. Kim, S. Kim, H.-T. Ha, and S. Kim, "Smartphone-based image analysis coupled to paper-based colorimetric devices," *Current Appl. Phys.*, vol. 20, no. 9, pp. 1013–1018, Sep. 2020. doi: 10.1016/j.cap.2020.06.021.

[25] R. Meng et al., "Smartphone-based colorimetric detection platform using color correction algorithms to reduce external interference," *Spectrochim. Acta A Mol. Biomol. Spectrosc.*, vol. 316, Aug. 2024, Art. no. 124350, doi: 10.1016/j.saa.2024.124350.